Journal of Solid State Electrochemistry (2020) 24:2901–2906
https://doi.org/10.1007/s10008-020-04667-2

ORIGINAL PAPER

The sum is more than its parts: stability of MnFe oxide nanoparticles supported on oxygen-functionalized multi-walled carbon nanotubes at alternating oxygen reduction reaction and oxygen evolution reaction conditions

Dulce M. Morales[1,2] · Mariya A. Kazakova[3] · Maximilian Purcel[1] · Justus Masa[4] · Wolfgang Schuhmann[1]

Received: 11 April 2020 / Revised: 22 May 2020 / Accepted: 23 May 2020 / Published online: 1 June 2020

Abstract

Successful design of reversible oxygen electrocatalysts does not only require to consider their activity towards the oxygen reduction (ORR) and the oxygen evolution reactions (OER), but also their electrochemical stability at alternating ORR and OER operating conditions, which is important for potential applications in reversible electrolyzers/fuel cells or metal/air batteries. We show that the combination of catalyst materials containing stable ORR active sites with those containing stable OER active sites may result in a stable ORR/OER catalyst if each of the active components can satisfy the current demand of their respective reaction. We compare the ORR/OER performances of oxides of Mn (stable ORR active sites), Fe (stable OER active sites), and bimetallic $Mn_{0.5}Fe_{0.5}$ (reversible ORR/OER catalyst) supported on oxidized multi-walled carbon nanotubes. Despite the instability of Mn and Fe oxide for the OER and the ORR, respectively, $Mn_{0.5}Fe_{0.5}$ exhibits high stability for both reactions.

Keywords Manganese oxide · Iron oxide · Multi-walled carbon nanotubes · Electrocatalysis · Stability · Bifunctional oxygen electrodes

Dedicated to Prof. Fritz Scholz on the occasion of his 65th birthday

Electronic supplementary material The online version of this article (https://doi.org/10.1007/s10008-020-04667-2) contains supplementary material, which is available to authorized users.

✉ Dulce M. Morales
dulce.moraleshernandez@rub.de

✉ Wolfgang Schuhmann
wolfgang.schuhmann@rub.de

[1] Analytical Chemistry – Center for Electrochemical Sciences (CES), Faculty of Chemistry and Biochemistry, Ruhr University Bochum, Universitätsstr. 150, 44780 Bochum, Germany

[2] Present address: Helmholtz-Zentrum Berlin für Materialien und Energie GmbH, Nachwuchsgruppe Gestaltung des Sauerstoffentwicklungsmechanismus, Hahn-Meitner-Platz 1, 14109 Berlin, Germany

[3] Boreskov Institute of Catalysis, SB RAS, Lavrentieva 5, Novosibirsk 630090, Russia

[4] Department of Heterogeneous Reactions, Max Planck Institute for Chemical Energy Conversion, Stiftstraße 34-36, 45470 Mülheim an der Ruhr, Germany

Introduction

Development and commercialization of regenerative energy conversion technologies, such as rechargeable metal-air batteries or reversible electrolyzer-fuel cell devices, are presently challenged by a lack of electrochemically stable materials that are able to reversibly catalyze both the oxygen reduction (ORR) and the oxygen evolution (OER) reactions at low overpotentials. A typical strategy for the fabrication of bifunctional ORR/OER electrocatalytic materials consists in combining at least two types of active sites into a composite, one being highly active towards the ORR while the other exhibits high activity towards the OER, resulting in highly active bifunctional ORR/OER catalysts [1–5]. However, the widely demonstrated trade-off between activity and stability, that is, the fact that often highly active materials exhibit poor long-term stability and vice versa [6–8], is rarely taken in consideration during catalyst design. Although this is an issue that concerns electrocatalysis in general, bifunctional electrocatalysis faces an even more daunting challenge: it requires the use of not only highly active but also highly stable

catalytic materials able to operate in the long term at the conditions of not one but of two different reactions.

Investigation of electrochemical stability of bifunctional ORR/OER catalysts is often demonstrated in the literature at either ORR or OER conditions [9–13]. While this approach could indicate the suitability of the materials for either ORR or OER applications, it does not provide information about their applicability as reversible oxygen electrodes. Thus, a proper assessment of the stability of bifunctional ORR/OER catalysts aiming to reversible energy conversion applications requires the observation of time-dependent electrocatalytic behavior at alternating reaction conditions. This, however, results often in a fast and severe damage of ORR active sites during the reaction conditions of the OER, and/or vice versa, after a short time of exposure to the two reactions [14–19].

Taking into account the aforementioned considerations, we propose as a strategy for the design of reversible ORR/OER electrodes the combination of an active ORR catalyst inherently stable within the potential range of ORR operation, with an active OER catalyst inherently stable within the potential range of OER operation. If the active sites of the former are able to satisfy the current demand of the electrochemical system during the ORR, it will kinetically govern the catalytic process without the aid of the latter, resulting in the protection of its active sites, and vice versa (Scheme 1).

Experimental

Catalyst synthesis and characterization

Synthesis of MO_X/MWCNTs-Ox-type catalysts has been reported previously [20]. In brief, growing of multi-walled carbon nanotubes (MWCNTs) was conducted by chemical vapor deposition of ethylene at a temperature of 680 °C using an Fe-Co growth catalyst [21, 22]. The majority of catalyst residues were removed by treating the MWCNTs in a boiling aqueous HCl solution (15 vol%) for 4 h under strong stirring [23], after which the MWCNTs were washed with distilled water until neutral pH. The dried MWCNTs were then treated in concentrated HNO_3 for 2 h while constantly stirring the mixture to introduce oxygen functionalities [24]. Subsequently, the oxygen-functionalized MWCNTs (MWCNTs-Ox) were washed with distilled water until neutral pH. After drying in air, MWCNTs-Ox were modified with Mn and Fe via incipient wet impregnation for 12 h using aqueous solutions of either $Fe(NO_3)_3$, $Mn(NO_3)_2$ as precursors, or a mixture of them at a 1:1 molar ratio. The impregnated materials were dried at 110 °C for 4 h and subsequently annealed under argon flow at 350 °C for 4 h to form the metal oxide nanoparticles. The overall metal loading of the catalysts was about 14 wt%.

Structural characterization has been reported previously [3, 20] and is summarized in Table S1.

Complementary Raman spectroscopy measurements were conducted with a Jubin-Yvon iHR550 spectrometer (HORIBA) equipped with a laser source of λ = 532 nm (Ventus 532, Laser Quantum) and a laser power of 2 mW.

N_2 adsorption isotherms, used for the determination of specific surface area, were obtained at a temperature of 77 K using an ASAP-2400 instrument (Micromeritics).

Electrochemical characterization

Electrochemical experiments were conducted in a three-electrode configuration rotating disk electrode setup using an Autolab PGSTAT128N potentiostat/galvanostat (Metrohm) equipped with an RDE 80793 rotator (Metrohm). Catalyst inks were prepared by dispersing 5 mg mL^{-1} active material in a mixture of water, ethanol, and Nafion (49:49:2 volume ratio) for 15 min via sonication. Glassy carbon rotating disk electrodes (RDEs) of 0.113 cm^2 geometric area were polished using 0.05 μm Al_2O_3 paste, and subsequently cleaned by placing them in a mixture of ethanol and water (1:1 volume ratio) followed by ultrasonication for 1 min. The RDEs were modified by drop-casting 4.8 μL catalyst ink to achieve a total catalyst loading of 210 μg cm^{-2}. After drying at room temperature under static air, the modified RDEs were used as the working electrode. A platinum mesh maintained during the measurements in a compartment separated by a glass frit was used as counter electrode. The reference electrode was a double-junction Ag/AgCl/KCl (3 M) electrode (Metrohm). An aqueous 0.1 M KOH solution saturated with oxygen was

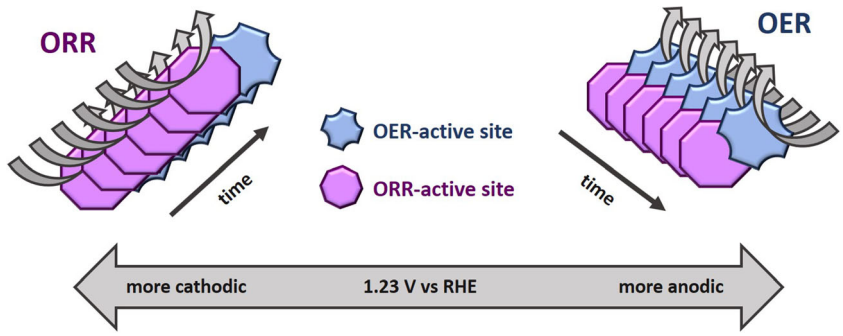

Scheme 1 Representation of the protection effect of active sites over time in reversible ORR/OER catalysts

used as the electrolyte. Prior to measurements, metal impurities contained in the electrolyte were removed by means of a Chelex cation-exchange resin (Bio-Rad Laboratories) [25]. After setup and before all measurements, the electrodes were subjected to continuous potential cycling between − 0.6 and 0.5 V vs. Ag/AgCl/KCl (3 M) at a scan rate of 100 mV s^{-1} until a constant response was observed. Subsequently, an electrochemical impedance spectrum (EIS) was recorded at open circuit potential in the frequency range between 100 kHz and 10 Hz with an AC amplitude of 10 mV (RMS) for the determination of the uncompensated resistance.

The electrocatalytic activity of the investigated catalysts towards the ORR and the OER was evaluated by means of RDE voltammetry by recording linear sweep voltammograms in the potential range from 0.1 to − 0.9 V vs. Ag/AgCl/KCl (3 M), and from 0.0 to 0.8 V vs. Ag/AgCl/KCl (3 M), respectively, with a scan rate of 5 mV s^{-1} and an electrode rotation of 1600 rpm. Activity measurements were done in triplicate and the average of the three measurements was reported.

Stability tests were conducted chronopotentiometrically in an RDE setup for 60 min by alternatingly applying two current densities, switching from one to the other each 2 min, while maintaining an electrode rotation of 1600 rpm. The current densities applied were 0 and − 1 mA cm^{-2}, 0 and + 10 mA cm^{-2}, or − 1 and + 10 mA cm^{-2}, to assess the stability during ORR, OER, and reversible ORR/OER, respectively. The applied currents were held for 5 s before start recording the electrode potentials.

Taking the pH of the electrolyte, the current measured (i), and the uncompensated resistance (R_u) into consideration, all measured potentials were iR_u-drop corrected and converted to the RHE scale according to Eq. 1.

$$E_{RHE} = E_{Ag/AgCl/KCl} + 0.207 + 0.059 \cdot pH - iR_u \quad (1)$$

The pH of the electrolyte was determined with a CP-411 pH-meter (Elmetron). R_u was extracted from the Nyquist plots obtained from EIS measurement for each electrode film.

Results and discussion

To demonstrate the proposed hypothesis, the electrochemical stability of oxides of Mn and Fe supported on oxygen-functionalized multi-walled carbon nanotubes, hereafter denoted as MnO_X/MWCNTs-Ox and FeO_X/MWCNTs-Ox, respectively, was investigated. Synthesis and characterization of the two catalysts have been previously reported [3, 20] and are summarized in Table S1. The catalysts were subjected to three different chronopotentiometric protocols to evaluate their stability at either (i) only OER, (ii) only ORR, or (iii) alternating ORR/OER conditions by applying alternately two current densities, each for 2 min, maintaining the alternation for a total of 1 h. The current densities applied were (i) + 10 and 0 mA cm^{-2} (only OER); (ii) − 1 and 0 mA cm^{-2} (only ORR); and (iii) − 1 and + 10 mA cm^{-2} (alternating ORR/OER). All stability tests were conducted in triplicate. The individual measurements (Fig. S1) and a short discussion concerning reproducibility have been included in the Supporting Information. Figure 1 a and b show the electrode potentials recorded for MnO_X/MWCNTs-Ox and FeO_X/MWCNTs-Ox, respectively, as a function of time, and are displayed with the same scale to facilitate comparison between ORR and OER overpotentials exhibited by the two catalysts. As shown in Fig. 1a, MnO_X/MWCNTs-Ox displayed a substantial deactivation during the only OER stability test, with an increase of overpotential of about 160 mV after 1 h. In contrast, the same catalyst exhibited a stable behavior during only ORR, with no substantial change of the measured potential throughout the measurement. The response observed during the stability test in which ORR and OER were conducted alternately did not differ considerably from those in which ORR and OER were done independently. In contradistinction, FeO_X/MWCNTs-Ox exhibited a more stable response than MnO_X/MWCNTs-Ox during the only OER stability measurement, with an increase of overpotential of less than 20 mV after 1 h, whereas an increase of ORR overpotential of less than 20 mV was observed by the end of the only ORR stability test (Fig. 1b). However, the response observed for FeO_X/MWCNTs-Ox when alternating between the ORR and OER displayed a considerably larger deactivation for both the OER and ORR, with increasing overpotentials of about 90 and 40 mV, respectively, after 1 h.

Linear sweep voltammograms of MnO_X/MWCNTs-Ox and FeO_X/MWCNTs-Ox were recorded before and after ORR/OER stability test and are shown in Fig. 1 c and d, respectively. The potentials recorded at current density values of − 1 mA cm^{-2} (E_{ORR}) and + 10 mA cm^{-2} (E_{OER}), as well as the difference between these two ($\Delta E = E_{OER} - E_{ORR}$), were found to be in agreement with those observed during the first ORR/OER alternation in the stability measurements (Table S2). To facilitate the comparison of the activity of these materials with other ORR and bifunctional ORR/OER catalysts reported in the literature, the potentials at which a current density of − 3 mA cm^{-2} was achieved and the resulting ΔE values are shown in Table S3. Voltammograms recorded at the end of the stability test displayed a clear increase in overpotential towards both the OER and the ORR. Discrepancies between E_{ORR} and E_{OER} values from the voltammograms and those from the last cycle of their corresponding chronopotentiometric measurements may be due to, e.g., an increase of damage of active sites, partial catalyst detachment, and accumulation of oxygen gas bubbles on the electrode surface [26].

The stability measurements showed that both MnO_X/MWCNTs-Ox and FeO_X/MWCNTs-Ox perform poorly as reversible ORR/OER catalysts. Nevertheless, MnO_X/

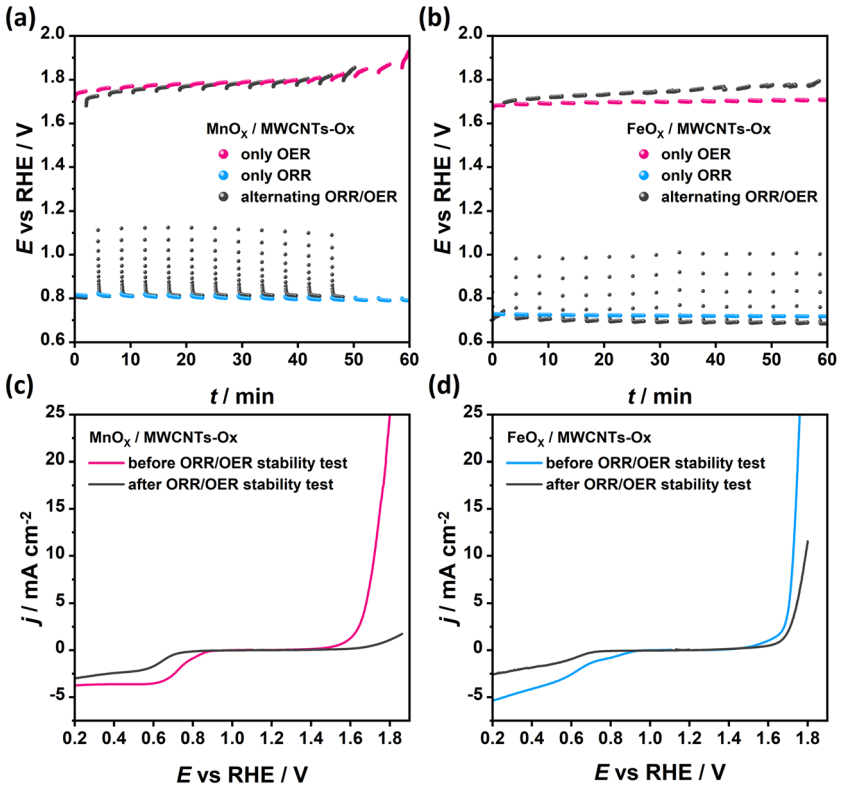

Fig. 1 Stability of **a** MnO_X/MWCNTs-Ox and **b** FeO_X/MWCNTs-Ox measured chronopotentiometrically by alternating each 2 min either between − 1 and 0 mA cm^{-2} (only ORR), between 10 and 0 mA cm^{-2} (only OER), or between − 1 and 10 mA cm^{-2} (alternating ORR/OER), for a total duration of 1 h. Data recorded at 0 mA cm^{-2} is not shown. Linear sweep voltammograms of **c** MnO_X/MWCNTs-Ox and **d** FeO_X/MWCNTs-Ox recorded at 5 mV s^{-1} scan rate before and after the alternating stability test. All measurements were conducted in O_2-staurated 0.1 M KOH with an electrode rotation of 1600 rpm

MWCNTs-Ox showed comparatively higher stability during the ORR than FeO_X/MWCNTs-Ox, and vice versa, FeO_X/MWCNTs-Ox displayed a more stable response than MnO_X/MWCNTs-Ox during the OER. According to the proposed hypothesis, a combination of the two catalysts, one being stable for ORR and the other being stable for OER, would result in a bifunctional catalyst of superior stability at alternating ORR/OER conditions as compared with that of its monometallic components. Consequently, we used the bimetallic catalyst $Mn_{0.5}Fe_{0.5}O_X$/MWCNTs-Ox in the same chronopotentiometric stability tests. As shown in Fig. 2a, increases in OER and ORR overpotentials of about 30 and 25 mV, respectively, were observed after 1 h, regardless of whether the ORR and OER were conducted separately or alternately. Linear sweep voltammograms recorded before and after ORR/OER stability measurements are shown in Fig. 2b demonstrating the superior stability of $Mn_{0.5}Fe_{0.5}O_X$/

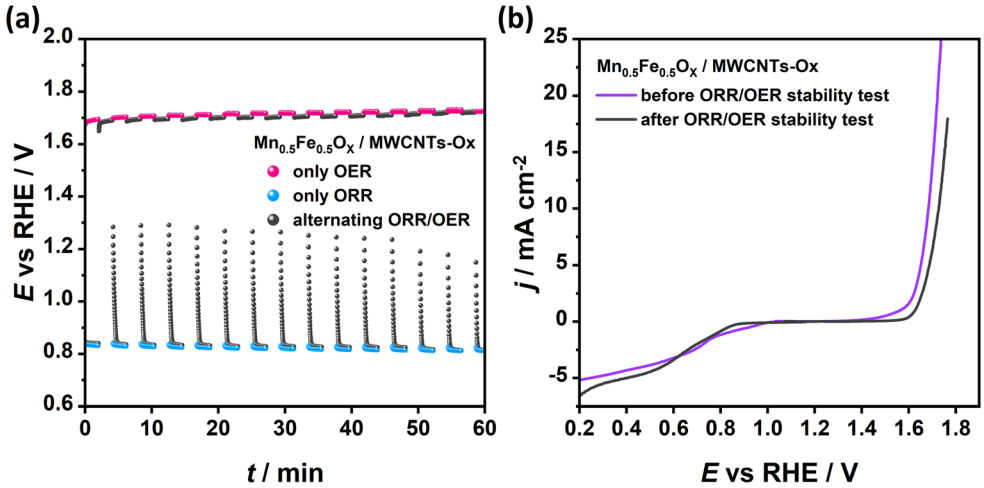

Fig. 2 **a** Stability of $Mn_{0.5}Fe_{0.5}O_X$/MWCNTs-Ox measured chronopotentiometrically by alternating each 2 min either between − 1 and 0 mA cm^{-2} (only ORR), between 10 and 0 mA cm^{-2} (only OER), or between − 1 and 10 mA cm^{-2} (alternating ORR/OER) for a total of 1 h. Data recorded at 0 mA cm^{-2} is not shown. **b** Linear sweep voltammograms recorded at 5 mV s^{-1} scan rate before and after stability test. All measurements were conducted in O_2-staurated 0.1 M KOH solution with an electrode rotation of 1600 rpm

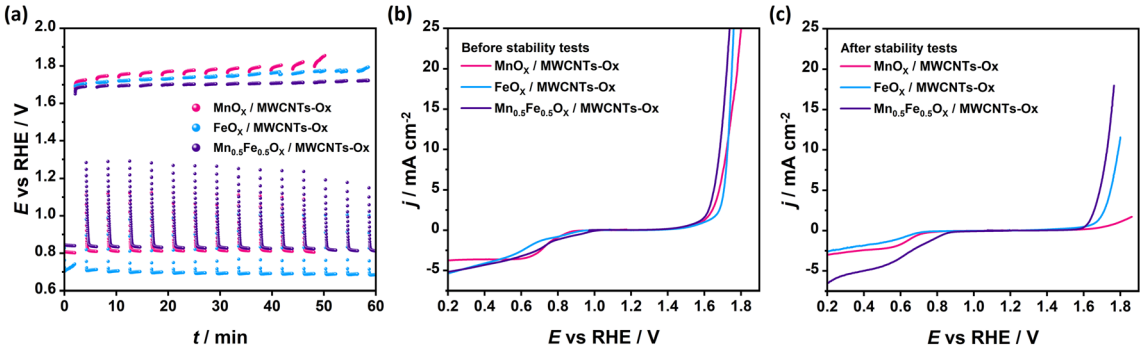

Fig. 3 Comparison of stability and activity of MO_X/MWCNTs-Ox, with M = Mn, Fe, and $Mn_{0.5}Fe_{0.5}$. **a** Electrochemical stability measured chronopotentiometrically by alternating each 2 min between − 1 and + 10 mA cm^{-2} for a total of 1 h. Linear sweep voltammograms recorded at a scan rate of 5 mV s^{-1} **b** before and **c** after stability tests. All measurements were conducted in O_2-staurated 0.1 M KOH solution with an electrode rotation of 1600 rpm

MWCNTs-Ox as compared with that of MnO_X/MWCNTs-Ox and FeO_X/MWCNTs-Ox (Fig. 1 c and d, respectively).

A comparison between the ORR/OER performances in terms of stability and activity exhibited by the three investigated catalysts is shown in Fig. 3. The bimetallic catalyst $Mn_{0.5}Fe_{0.5}O_X$/MWCNTs-Ox exhibited not only a substantial higher stability, but also lower overpotentials for both the ORR and OER compared with the monometallic materials, both at the beginning and at the end of the stability measurements. The activity enhancement has been previously discussed [3] and is ascribable to the formation of more active catalytic sites, for instance $MnFe_2O_4$ (Table S1), as well as synergistic interactions upon combining the different metal components. The presence of more active catalytic sites seemed to facilitate the supply of current over time during the OER, whereas in the case of the ORR, the observed response did not differ substantially from that of MnO_X/MWCNTs-Ox as the measurement progressed. This observation indicates that MnO_X remained the main catalytic site for the ORR and was indeed able to satisfy the current demand for this reaction entirely, thus protecting the OER active sites from reductive damage. In the same way, due to the kinetic advantage of the OER catalytic sites, the ORR active sites were protected during the OER as long as the OER sites were able to provide the required current.

Conclusions

We propose a strategy for the design of reversible ORR/OER electrocatalyst by combining inherently stable ORR active sites with inherently stable OER active sites, each of them being capable to supply the current demand of the electrochemical system without the aid of the other. The strategy was demonstrated with the investigation of the electrochemical stability of Mn, Fe, and $Mn_{0.5}Fe_{0.5}$ oxides supported on oxidized multi-walled carbon nanotubes at alternating ORR/OER conditions. Mn oxide exhibited high stability during ORR, but its activity decreased fast when exposed to the highly anodic OER potentials. Fe oxide displayed a comparatively higher stability towards the OER than Mn oxide; however, a substantial increase of both ORR and OER overpotentials was observed at alternating ORR/OER conditions. In agreement with our hypothesis, $Mn_{0.5}Fe_{0.5}$ oxide exhibited a superior electrochemical stability than the monometallic catalysts at alternating ORR/OER. Although these results suggest that the stability enhancement is due to the kinetic advantage of OER active sites over ORR active sites during OER, or vice versa during ORR, structural characterization of the investigated catalysts at *operando* conditions is still required to fully reveal the nature of the observed stability enhancement.

Acknowledgments The authors are grateful to the Bundesministerium für Bildung und Forschung (BMBF). Mariya A. Kazakova ackowledges the Ministry of Science and Higher Education of the Russian Federation.

Code availability Not applicable (software application or custom code).

Funding information Open Access funding provided by Projekt DEAL. Mariya A. Kazakova received financial support by the Ministry of Science and Higher Education of the Russian Federation. The authors received financial support from the Bundesministerium für Bildung und Forschung (BMBF) in the frameworks of the project “Mangan” (FKZ 03EK3548).

Data availability All data are stored on a server with frequent backup.

Compliance with ethical standards

Conflict of interest The authors declare that they have no conflict of interest.

References

1. Rincon RA, Masa J, Mehrpour S, Tietz F, Schuhmann W (2014) Activation of oxygen evolving perovskites for oxygen reduction by functionalization with Fe-N_X/C groups. Chem Commun 50(94): 14760–14762
2. Zhong H, Tian R, Gong X, Li D, Tang P, Alonso-Vante N, Feng Y (2017) Advanced bifunctional electrocatalyst generated through cobalt phthalocyanine tetrasulfonate intercalated Ni_2Fe-layered double hydroxides for a laminar flow unitized regenerative micro-cell. J Power Sources 361:21–30
3. Morales DM, Kazakova MA, Dieckhöfer S, Selyutin AG, Golubtsov GV, Schuhmann W, Masa J (2020) Trimetallic Mn-Fe-Ni oxide nanoparticles supported on multi-walled carbon nanotubes as high-performance bifunctional ORR/OER electrocatalyst in alkaline media. Adv Funct Mater 30(6):1905992
4. Morales DM, Masa J, Andronescu C, Kayran YU, Sun Z, Schuhmann W (2016) Few-layer graphene modified with nitrogen-rich metallo-macrocyclic complexes as precursor for bifunctional oxygen electrocatalysts. Electrochim Acta 222:1191–1199
5. Masa J, Xia W, Sinev I, Zhao A, Sun Z, Grützke S, Weide P, Muhler M, Schuhmann W (2014) Mn_xO_y/NC and Co_xO_y/NC nanoparticles embedded in a nitrogen-doped carbon matrix for high-performance bifunctional oxygen electrodes. Angew Chem Int Ed 53(32):8508–8512
6. Barwe S, Andronescu C, Masa J, Schuhmann W (2017) The two Janus faces in oxygen evolution electrocatalysis: activity versus stability of layered double hydroxides. Curr Opin Electrochem 4(1):4–10
7. Chang SH, Connell JG, Danilovic N, Subbaraman R, Chang K-C, Stamenkovic VR, Markovic NM (2014) Activity-stability relationship in the surface electrochemistry of the oxygen evolution reaction. Faraday Discuss 176:125–133
8. Danilovic N, Subbaraman R, Chang K-C, Chang SH, Kang YJ, Snyder J, Paulikas AP, Strmcnik D, Kim Y-T, Myers D, Stamenkovic VR, Markovic NM (2014) Activity-stability trends for the oxygen evolution reaction on monometallic oxides in acidic environments. J Phys Chem Lett 5(14):2474–2478
9. Elumeeva K, Masa J, Tietz F, Yang F, Xia W, Muhler M, Schuhmann W (2016) A simple approach towards high-performance perovskite-based bifunctional oxygen electrocatalysts. Chem Electro Chem 3(1):138–143
10. Li Y, Kuttiyiel KA, Wu L, Zhu Y, Fujita E, Adzic RR, Sasaki K (2017) Enhancing electrocatalytic performance of bifunctional cobalt-manganese-oxynitride nanocatalysts on graphene. ChemSusChem 10(1):68–73
11. Zhao Y, Kamiya K, Hashimoto K, Nakanishi S (2015) Efficient bifunctional Fe/C/N electrocatalysts for oxygen reduction and evolution reaction. J Phys Chem C 119(5):2583–2588
12. Kim N-I, Sa YJ, Yoo TS, Choi SR, Afzal RA, Choi T, Seo Y-S, Lee K-S, Hwang JY, Choi WS, Joo SH, Park J-Y (2018) Oxygen-deficient triple perovskites as highly active and durable bifunctional electrocatalysts for oxygen electrode reactions. Sci Adv 4(6): eaap9360
13. Ahmed MS, Choi B, Kim Y-B (2018) Development of highly active bifunctional electrocatalyst using Co_3O_4 on carbon nanotubes for oxygen reduction and oxygen evolution. Sci Rep 8(1):2543
14. Prabu M, Ramakrishnan P, Shanmugam S (2014) $CoMn_2O_4$ nanoparticles anchored on nitrogen-doped graphene nanosheets as bifunctional electrocatalyst for rechargeable zinc–air battery. Electrochem Commun 41:59–63
15. Morales DM, Masa J, Andronescu C, Schuhmann W (2017) Promotional effect of Fe impurities in graphene precursors on the activity of MnO_X/graphene electrocatalysts for the oxygen evolution and oxygen reduction reactions. Chem Electro Chem 4(11): 2835–2841
16. Kazakova MA, Morales DM, Andronescu C, Elumeeva K, Selyutin AG, Ishchenko AV, Golubtsov GV, Dieckhöfer S, Schuhmann W, Masa J (2019) Fe/Co/Ni mixed oxide nanoparticles supported on oxidized multi-walled carbon nanotubes as electrocatalysts for the oxygen reduction and the oxygen evolution reactions in alkaline media. Catal Today. https://doi.org/10.1016/j.cattod.2019.02.047
17. Dresp S, Luo F, Schmack R, Kühl S, Gliech M, Strasser P (2016) An efficient bifunctional two-component catalyst for oxygen reduction and oxygen evolution in reversible fuel cells, electrolyzers and rechargeable air electrodes. Energy Environ Sci 9(6):2020–2024
18. Silva RA, Soares CO, Afonso R, Carvalho MD, Tavares AC, Melo Jorge ME, Gomes A, da Silva Pereira MI, Rangel CM (2017) Synthesis and electrocatalytic properties of $La_{0.8}Sr_{0.2}FeO_{3-\delta}$ perovskite oxide for oxygen reactions. AIMS Mater Sci 4(4):991–1009
19. McKerracher RD, Figueredo-Rodríguez HA, Ponce de León C, Alegre C, Baglio V, Aricò AS, Walsh FC (2016) A high-performance, bifunctional oxygen electrode catalysed with palladium and nickel-iron hexacyanoferrate. Electrochim Acta 206:127–133
20. Elumeeva K, Kazakova MA, Morales DM, Medina D, Selyutin A, Golubtsov G, Ivanov Y, Kuznetzov V, Chuvilin A, Antoni H, Muhler M, Schuhmann W, Masa J (2018) Bifunctional oxygen reduction/oxygen evolution activity of mixed Fe/Co oxide nanoparticles with variable Fe/Co ratios supported on multiwalled carbon nanotubes. Chem Sus Chem 11(7):1204–1214
21. Bokova-Sirosh SN, Kuznetsov VL, Romanenko AI, Kazakova MA, Krasnikov DV, Tkachev EN, Yuzyuk YI, Obraztsova ED (2016) Investigation of defectiveness of multiwalled carbon nanotubes produced with Fe–Co catalysts of different composition. J Nanophoton 10(1):12526
22. Andreev AS, Krasnikov DV, Zaikovskii VI, Cherepanova SV, Kazakova MA, Lapina OB, Kuznetsov VL, d'Espinose de Lacaillerie J–B (2018) Internal field 59Co NMR study of cobalt-iron nanoparticles during the activation of $CoFe_2$/CaO catalyst for carbon nanotube synthesis. J Catal 358:62–70
23. Kuznetsov VL, Elumeeva KV, Ishchenko AV, Beylina NY, Stepashkin AA, Moseenkov SI, Plyasova LM, Molina IY, Romanenko AI, Anikeeva OB, Tkachev EN (2010) Multi-walled carbon nanotubes with ppm level of impurities. Phys Status Solidi B 247(11-12):2695–2699
24. Kazakova MA, Andreev AS, Selyutin AG, Ishchenko AV, Shuvaev AV, Kuznetsov VL, Lapina OB, d'Espinose de Lacaillerie J-B (2018) Co metal nanoparticles deposition inside or outside multi-walled carbon nanotubes via facile support pretreatment. Appl Surf Sci 456:657–665
25. Wuttig A, Surendranath Y (2015) Impurity ion complexation enhances carbon dioxide reduction catalysis. ACS Catal 5(7):4479–4484
26. Zeradjanin AR (2018) Frequent pitfalls in the characterization of electrodes designed for electrochemical energy conversion and storage. Chem Sus Chem 11(8):1278–1284